



HAL
open science

Biomechanical evaluation of Back injuries during typical snowboarding backward falls

Wei Wei, Morgane Evin, Nicolas Bailly, Pierre-jean Arnoux

► To cite this version:

Wei Wei, Morgane Evin, Nicolas Bailly, Pierre-jean Arnoux. Biomechanical evaluation of Back injuries during typical snowboarding backward falls. *Scandinavian Journal of Medicine and Science in Sports*, 2023, 33 (3), pp.224-234. 10.1111/sms.14254 . hal-04050199

HAL Id: hal-04050199

<https://hal.science/hal-04050199v1>

Submitted on 28 Apr 2023

HAL is a multi-disciplinary open access archive for the deposit and dissemination of scientific research documents, whether they are published or not. The documents may come from teaching and research institutions in France or abroad, or from public or private research centers.

L'archive ouverte pluridisciplinaire **HAL**, est destinée au dépôt et à la diffusion de documents scientifiques de niveau recherche, publiés ou non, émanant des établissements d'enseignement et de recherche français ou étrangers, des laboratoires publics ou privés.



Distributed under a Creative Commons Attribution - NonCommercial 4.0 International License

Biomechanical evaluation of Back injuries during typical snowboarding backward falls

Wei Wei^{1,2} | Morgane Evin^{1,2} | Nicolas Bailly^{1,2} | Pierre-Jean Arnoux^{1,2}

¹LBA UMRT24, Aix Marseille Université/Université Gustave Eiffel, Marseille, France

²iLab-Spine - Laboratoire International en Imagerie et Biomécanique du Rachis, Marseille, France

Correspondence

Wei Wei, Laboratoire de Biomécanique Appliquée, Bd. P. Dramard, Faculté de Médecine secteur-Nord, France 13916 Marseille cedex 20, France.
Email: wei.wei@univ-eiffel.fr

To prevent spinal and back injuries in snowboarding, back protector devices (BPDs) have been increasingly used. The biomechanical knowledge for the BPD design and evaluation remains to be explored in snowboarding accident conditions. This study aims to evaluate back-to-snow impact conditions and the associated back injury mechanisms in typical snowboarding backward falls. A previously validated snowboarder multi-body model was first used to evaluate the impact zones on the back and the corresponding impact velocities in a total of 324 snowboarding backward falls. The biomechanical responses during back-to-snow impacts were then evaluated by applying the back-to-snow impact velocity to a full human body finite element model to fall on the snow ground of three levels of stiffness (soft, hard, and icy snow). The mean values of back-to-snow normal and tangential impact velocities were 2.4 m/s and 7.3 m/s with maximum values up to 4.8 m/s and 18.5 m/s. The lower spine had the highest normal impact velocity during snowboarding backward falls. The thoracic spine was found more likely to exceed the limits of flexion-extension range of motions than the lumbar spine during back-to-snow impacts, indicating a higher injury risk. On the hard and icy snow, rib cage and vertebral fractures were predicted at the costal cartilage and the posterior elements of the vertebrae. Despite the possible back injuries, the back-to-snow impact force was always lower than the force thresholds of the current BPD testing standard. The current work provides additional biomechanical knowledge for the future design of back protections for snowboarders.

KEYWORDS

back protection, biomechanics, finite element, multi-body, snowboarding

Abbreviations: α , The steepness of the snow slope; β , The initial body posture of the snowboarder; H , The snowboarder anthropometry; θ , The angle of the snowboarding approach; S_{snow} , The stiffness of the snow; V_0 , Snowboarding initial velocity before the fall; ANOVA, Analysis of variance; BPD, Back protector device; EPS, Effective plastic strain; FE, Finite element; FSU, Functional spinal unit; HSD, Honest significant difference; MB, Multi-body; ROM, Range of motions; SPI, Spinal injury; THUMS, Total human model for safety.

This is an open access article under the terms of the [Creative Commons Attribution-NonCommercial-NoDerivs](https://creativecommons.org/licenses/by-nc-nd/4.0/) License, which permits use and distribution in any medium, provided the original work is properly cited, the use is non-commercial and no modifications or adaptations are made.

© 2022 The Authors. *Scandinavian Journal of Medicine & Science In Sports* published by John Wiley & Sons Ltd.

1 | INTRODUCTION

The population of alpine skiing and snowboarding was about 50 million in France and 200 million in Europe during the past 5 years.¹ The corresponding number was more than 9 million in the 2017–2018 season in the United States.² Alpine skiing and snowboarding are generally high-energy outdoor winter sports with inherent risks which could result in grievous falls and collisions. The traumatic injuries were reported to occur at a rate of 1–5 per 1000 participant days.³ Skiing and snowboarding injuries accounted for 22.3% of sports injuries in Switzerland.⁴ Spinal injury (SPI) was found in 3.3% of snowboarding-related injuries and 1.4% of skiing-related injuries.⁵ SPI was also observed as the second most common cause (second only to traumatic brain injury) of severe and/or life-threatening traumatic injuries in skiing and snowboarding.⁶ The ratio of SPIs leading to complete tetraplegia or paraplegia in 2016 was estimated to be 33.3%.⁷

To prevent injuries to the spine and back, back protector devices (BPDs) have been increasingly used by snow sports participants. The ratios of skiers and snowboarders wearing BPDs in Switzerland were respectively 12% and 40% in the 2015–2016 season while only 2% and 7% in the 2002–2003 season.⁴ BPDs are designed to attenuate the shock to the back by distributing the impact force over a wider area of the back. However, no specific testing standard exists yet for BPDs of snow sports. The performance evaluation of snow sport BPDs is mostly based on the European testing standard EN1621-2⁸ which is originally designed for motorcyclist back protection. BPDs are stricken by a metal impactor with a kinetic energy of 50 J in the EN1621-2 standard and graded according to the impact force to BPDs. The BPD is certified as a level-1 (or level-2) device if the mean value of impact forces is not higher than 18 kN (or 9 kN) with the impact force of each strike no higher than 24 kN (or 12 kN). A few studies were performed previously to evaluate the performance of snow sport BPDs with experimental tests^{9,10} and to optimize the design of BPDs with numerical simulations.¹¹ These studies were based on the assumption that the current BPD testing standard⁸ should be effective to prevent or mitigate SPIs in snow sports. However, the back-to-snow impact conditions (e.g. impact velocity and impact position) and the associated mechanisms of back injuries during snow sports accidents have never been investigated.

Human body kinematics during typical snowboarding backward falls were previously simulated and analyzed with a multi-body (MB) simulation approach.¹² SPI risks were also estimated in terms of spinal flexion-extension range of motions (ROMs).¹² Back-to-snow

impact velocity was nevertheless not evaluated. Being unable to capture material deformation, the MB simulation approach cannot thus accurately compute the body impact force and the back-to-snow impact force was not consequently studied. Finite element (FE) modeling has been widely used to understand thoracic injury mechanisms in vehicle collisions^{13–15} and sports accidents.^{16,17} The thoracic responses of human FE models, such as impact force, chest deflection/compression, and viscous criterion, were usually used as metrics to predict the likelihood of thoracic injury.¹³ The localized organ responses (e.g. stress and strain on the spinal vertebrae and rib cage) of human FE models could help to determine the injury types and address the injury mechanisms.^{13–16} Human FE modeling may be promising in quantifying the biomechanical responses and predicting the corresponding injuries in snowboarding backward fall conditions.

Therefore, the objective of this study was twofold:

Firstly, to evaluate the back-to-snow impact conditions (e.g. impact velocity and impact position) in typical snowboarding backward falls with the MB approach.

Secondly, to quantify the biomechanical responses of the snowboarder during back-to-snow impacts with the FE approach.

2 | MATERIALS AND METHODS

This study consisted of four components (see Appendix A in the Appendix S1): (1) analysis of back-to-snow impact conditions with MB simulations of typical snowboarding backward falls, (2) human body FE model validation against blunt impacts to the back, (3) material characterization of snow with FE simulations of head-to-snow impact, and (4) back injury analysis during back-to-snow impacts with FE simulations.

2.1 | Snowboarder back-to-snow impact conditions with MB simulations

The human MB model (Figure 1) used to reconstruct typical snowboarding backward falls in our previous study¹² was chosen to evaluate the back-to-snow impact conditions in this study. To briefly review, the human MB model was previously calibrated against the spinal segment ROMs, and validated against the body dynamic responses in the vehicle-pedestrian collision and snowboarding backward fall conditions.¹² Similar to our previous study,¹² the human MB model was currently used to reproduce typical snowboarding backward falls of various initial accident conditions (Figure 1A): initial velocity

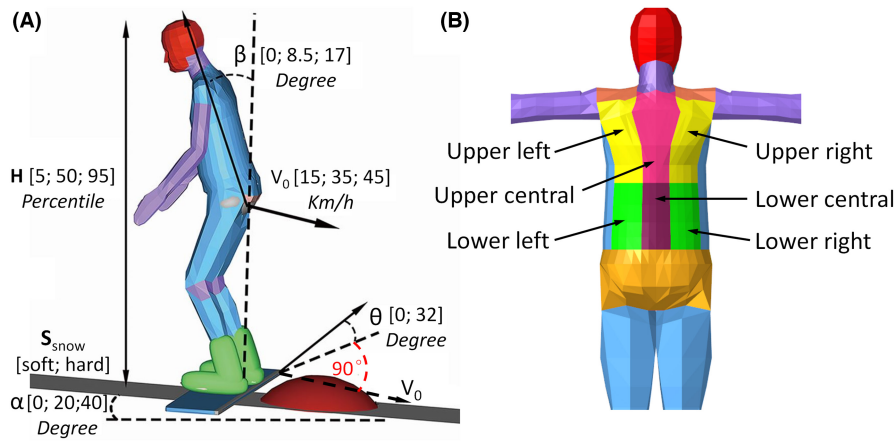


FIGURE 1 Multi-body model setup for snowboarding backward falls: (A) parametric analysis on back impact velocity during diverse snowboarding backward falls; (B) divisions of different back regions. H , anthropometry; S_{snow} , snow stiffness; V_0 , initial velocity; α , slope steepness; β , body posture; θ , approach angle

(V_0), slope steepness (α), body posture (β), angle of approach (θ), anthropometry (H), and snow stiffness (S_{snow}). The variation levels of these initial conditions were summarized in Figure 1A and were chosen according to our previous study.¹² Among the initial accident variables, the body posture was defined as the spinal flexion angle (C0-sacrum) relative to the neutral posture of the human MB model. The angle of approach was the angle between the snowboard and the perpendicular direction to the initial velocity (i.e. the angle between the snowboard and initial velocity minus 90°). The three velocity levels (i.e. 15 km/h, 35 km/h, and 45 km/h) represent the average velocities of beginner, intermediate, and good snowboarders^{18,19} while the slope angles (i.e. 0°, 20°, and 40°) represent the typical easy and medium ski slopes.²⁰ A total of 324 snowboarding backward falls were simulated to constitute the full factorial design of the experiments.

The back surface of the snowboarder was divided into six areas (displayed in Figure 1B) to represent the critical regions (i.e. upper and lower central), impacts to which might involve SPIs, and the less critical ones. The number of cases in which the snowboarder collided with the snow ground on the back was counted. For the cases with back-to-snow collisions, the back region firstly hitting the ground was subsequently analyzed. The velocity of the back at the first moment of back-to-snow collision (hereafter referred to as “back-to-snow velocity” for simplicity) was also evaluated. All the MB simulations were performed with MADYMO R7.5 (TASS; Delft, the Netherlands).

Bartlett's test was used to identify whether the back-to-snow velocities have equal variances across different groups of the back regions firstly hitting the ground. The student's t -test was used to assess the difference of back-to-snow velocities between every two back regions. After data normality and homogeneity were confirmed with Shapiro–Wilk and Bartlett tests, one-way analysis of variance (ANOVA) and Tukey's honest significant difference (HSD) test were performed to identify the initial condition variables and the variables' levels having significant

effects on back-to-snow velocities. Statistical significance was defined as a two-tailed p -value <0.10 while considering different significance levels with p -value less than 0.001, 0.01, 0.05, or 0.1. The statistical analysis was performed with the software Rstudio 1.2 (Rstudio, Inc.).

2.2 | Back impact validation of human body FE model

The Total Human Model for Safety (THUMS) v5.03AM50 (1.78 m, 78.2 kg) occupant model was chosen to represent the mid-size snowboarder and to study injuries during snowboarding backward falls. The THUMS model is a human body FE model intended to reproduce human body kinematics and injuries during vehicle crash accidents.^{21,22} The biomechanical responses of the THUMS model have been validated on the scales of the organs (e.g. lung, spleen, and liver), body regions (e.g. head/ brain, neck, thorax, and extremities), and on the scale of the whole body for various automobile impact conditions.²³ However, to our knowledge, the THUMS model had never been validated against blunt impacts to the back. To use the THUMS model for back injury analysis in snowboarding backward falls, the model was first validated against experimental blunt impacts to the back^{24,25} which were assumed to be relevant to the loading conditions in snowboarding backward falls. The model validation procedure and results were detailed in Appendix B in the Appendix S1.

2.3 | Modeling of the snow

The mechanical properties of the snow in dynamic loadings were characterized in this study since these data were not directly available in the literature for the explicit solver of LS-DYNA (LSTC). FE simulations were performed to reproduce previous experimental drop tests in which a 6 kg metallic head form was released from three heights to

hit soft and hard snow with initial velocities of 5.44 m/s, 6.25 m/s, and 7.67 m/s.²⁰ The constitutive model of viscous foam was chosen to model the mechanical behavior of soft and hard snow. A multi-objective optimization approach was used to obtain the optimal material coefficients of the soft and hard snow by mapping the head acceleration time histories of simulations to those of the experimental tests. The FE simulation setup and the optimization-based procedure were detailed in Appendix C in the Appendix S1. The optimal material coefficients of the soft and hard snow were also displayed in Figure C2 in Appendix C. With the optimal coefficients of the snow, the resultant accelerations of the head form in the simulations matched well with the experimental measurements for the three impact velocities (see Figure C2 in Appendix C.), in particular in terms of the peak values and the trends of the curves.

2.4 | Snowboarder back-to-snow impact FE simulations

The snowboarder biomechanical responses in typical backward falls were finally evaluated by performing back-to-snow impact FE simulations. The mid-size THUMS model which was above validated against blunt back impacts (in section 2.2) was used here to model the snowboarder. The snowboarder was pre-positioned close to a supine position with the back slightly above a layer of snow (Figure 2). The layer

of snow had the same size (1000 mm * 1000 mm * 300 mm) as that used in the snow modeling section (section 2.3 and Appendix C). Similarly, the snow layer was modeled with 6-node hexahedron elements and was fixed on its bottom surface. The superior surface of the snow was slightly modified to represent a groomed slope with a flat surface and to represent a bumpy slope with a spherical bump surface (SR = 100 mm and h = 30 mm) (Figure 2). The back impact on the spherical bump surface was performed at three positions: at T8 (the eighth thoracic vertebra), T12 (the twelfth thoracic vertebra), L2 (the second lumbar vertebra), and L4 (the fourth lumbar vertebra) level (Figure 2). Three levels of stiffness were simulated for the snow ground: soft and hard snow (material coefficients obtained in section 2.3 and displayed in Figure C2 in Appendix C), and completely rigid to model either a concrete floor or ice.

The snowboarder FE model was applied with an initial velocity of 2.4 m/s along the vertical direction corresponding to the mean value of back-to-snow normal impact velocities obtained in snowboarder backward fall MB simulations (see section 2.1 and result section 3.1). The back impact force was measured as the contact force between the back and the snow. With a similar method as in section 2.2 of back impact validation (see Figure B1 in Appendix B), the back deflection was measured as the change in length between a node on the thoracoabdominal skin and a node on the back skin at T8, T12, L2, and L4 for all the simulations. The back compression was computed

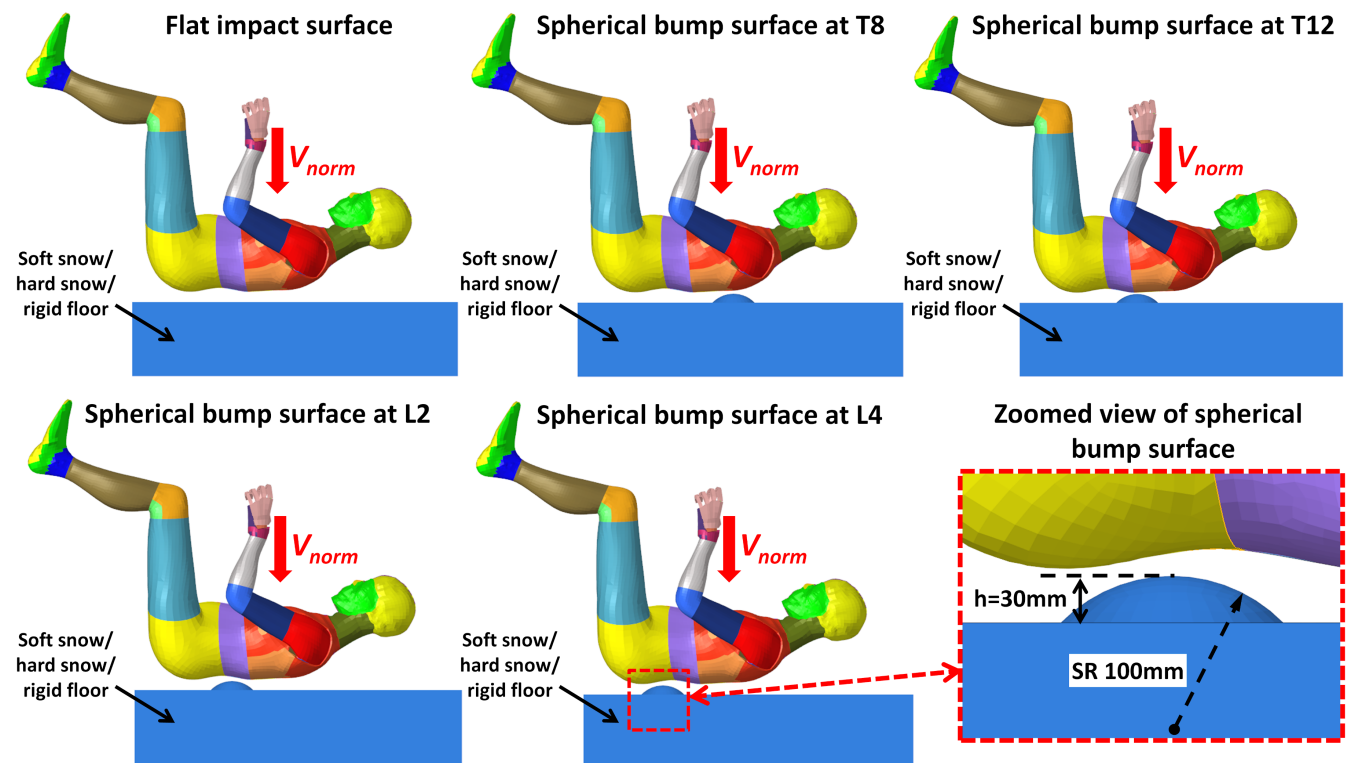


FIGURE 2 Model setup of back-to-snow impact FE simulation for back injury analysis

by dividing the back deflection by the corresponding initial chest depth (i.e. 232 mm at T8, 231 mm at T12, 243 mm at L2, and 251 mm at L4). The vertebral impact loadings and the flexion-extension ROM of each functional spinal unit (FSU) were also evaluated during the back-to-snow impact.

The back-to-snow impact was simulated for a duration of 100 ms to fully capture the first impact between the back and snow, and to save calculation expenses. A total of 15 back-to-snow impact simulations were performed to take into account three types of snow stiffness, two impact surfaces, and four impact positions on the back (Figure 2).

All the FE simulations in this study were performed with the explicit solver in LS-DYNA 971 R11.1 (LSTC, Livermore, CA, USA) on an Intel Xeon (2.20 GHz) workstation with 24 processors.

3 | RESULTS

3.1 | Snowboarder back-to-snow impact conditions: MB simulations

Among the 324 snowboarding backward falls, the back hit the snow ground in 263 (81.2%) cases (Table 1). Among the 263 back-to-snow impact cases, the back region hitting the snow ground firstly was most frequently located at the upper lateral back (region-1), followed by the lower lateral back (region-3), lower central back (region-4), and higher central back (region-2) (Table 1). Displayed in Figure 3 were the back-to-snow impact velocities for each divided back region. The mean values of the normal and tangential back-to-snow impact velocities were respectively 2.4 m/s and 7.3 m/s. The lower central (3.0 m/s) hit the snow ground with a higher mean value of normal velocity than the upper lateral (2.2 m/s) and lower lateral (2.1 m/s) back (Figure 3). The opposite trend was found for the tangential back-to-snow velocity: the lower lateral (7.9 m/s) impacted the snow with a higher mean value than the lower central (6.1 m/s) back (Figure 3).

The effects of the initial accident variables on the impact velocity of the whole back were displayed in Figure 3. The initial velocity (V_0), the slope steepness (α), and the angle of approach (θ) were found to significantly affect the back-to-snow impact velocity. As these three variables (i.e. V_0 , α , θ) increased, the tangential and resultant back-to-snow velocities increased but the normal back-to-snow velocity decreased (Figure 4).

3.2 | Back injuries during back-to-snow impacts: FE simulations

Displayed in Appendix D (in the Appendix S1) was the normalized flexion-extension angle of each thoracolumbar

FSU, which was calculated by dividing the FSU flexion-extension ROMs of the simulations by the previously reported FSU flexion-extension thresholds.¹² Among all the backward falls, only the impacts to the rigid bump surface at T8, T12, and L2 levels had a normalized flexion-extension angle higher than 100% (Figure D1 in Appendix D), indicating a likely injury at the corresponding FSUs. The FSUs of a normalized flexion-extension angle higher than 100% were always close to the spinal levels impacted on the rigid bump surface: T8-T9 for rigid bump impact at T8; T12-L1 for rigid bump impacts at T12 and L2.

The back compressions measured at T8, T12, L2, and L4, as well as the back impact force of the simulations, were summarized as the peak values in Table 2. For all the backward falls, the back compressions ranged from 14.9% to 32.0% with the highest compression (32.0%) measured at the T8 level for the rigid bump impact at T8 and the lowest compression (14.9%) at the L4 level in the soft snow bump impact at L4. The back impact forces ranged from 5.06 kN to 7.92 kN with the highest force (7.92 kN) also measured in the rigid bump impact at T8 and the lowest force (5.06 kN) measured in the impact on the flat soft snow surface. In 10 cases, the effective plastic strain (EPS) of the rib cage cortical bones exceeded the pre-defined threshold of 2.4% indicating a fracture (Table 2 and Figure 5). The rib fracture always occurred in the costal cartilage (Figure 5).


The peak values of EPS and the corresponding spinal vertebra levels were summarized in Table E1 (in Appendix E in the Appendix S1). The cortical bones at the L1 level sustained an EPS higher than the previously proposed threshold²⁶ in the impacts on the flat rigid surface, the rigid bump at T12, and the hard snow bump at T12 (Figure 6). The cortical bones of the T9 vertebra in the rigid bump impact at T8 also had an excessive EPS (Figure 6). These excessive effective strains indicated the likely fractures at the cortical bones of the corresponding vertebral levels. The EPS of the spongy bones was always lower than the threshold proposed by Sterba et al.,²⁶ indicating the unlikely fracture at the spongy bones.

4 | DISCUSSION

4.1 | Snowboarder back-to-snow impact conditions

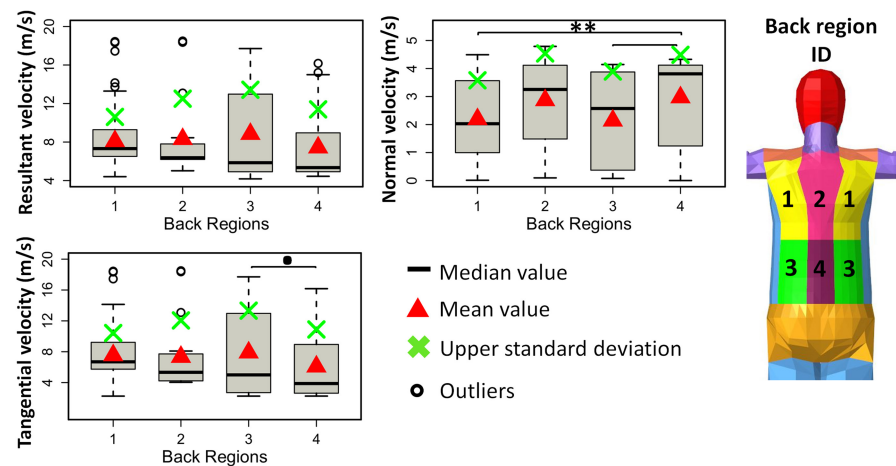
In the present study, the first back regions colliding with the snow ground and the corresponding back-to-snow impact velocities were evaluated with the snowboarder MB model. The upper back was found more frequently impacted (52.7%) than the lower back (28.4%). However, it was the lower central back that had the highest normal impact velocity (3.0 m/s). Interestingly, lumbar spinal fractures (34.5–69.4%)

TABLE 1 The first back regions impacting the snow with the corresponding frequencies and ratios: 1-upper left and right back, 2-upper central back, 3-lower left and right back, 4-lower central back

Region	0 ^a	1	2	3	4	Back region ID
Frequency	61	154	17	48	44	
Ratio (%)	18.8	47.5	5.2	14.8	13.6	

^a0 indicates that the back did not hit the ground during the falls.

FIGURE 3 Back-to-snow impact velocity grouped by different back regions: 1-upper left and right back, 2-upper central back, 3-lower left and right back, 4-lower central back. *p* values: ****p* < 0.001, ***p* < 0.01, **p* < 0.05, *p* < 0.1



were found more frequently than thoracic spinal fractures (21.8–33.2%) in snowboarding-related spinal fractures in previous epidemiology studies.^{5,27} Snowboarding backward falls due to jump landing failure were reported as one of the leading mechanisms for spinal fractures among snowboarders.²⁸ The higher normal impact velocity of the lower central back estimated in this study might partially explain the higher frequency of lumbar spinal fractures than thoracic in snowboarding-related spinal fractures. This may also emphasize the necessity of higher-level protection for the lumbar spine of snowboarders.

Among the backward falls, the normal and tangential back-to-snow impact velocities were up to 4.8 m/s and 18.5 m/s respectively (Figure 3). In 255 (97%) backward falls, the normal back-to-snow impact velocity was lower than the impact velocity of 4.5 m/s applied in the current BPD testing standard.⁸ The normal and tangential impact velocities were significantly affected by the initial snowboarding speed, slope steepness, and angle of approach (Figure 4). Surprisingly, the lower the initial speed of snowboarding before backward falls, the higher the normal back-to-snow impact velocity, and hence the more vulnerable the snowboarder's back could be. This was because the head hit the snow first mostly during higher-speed (35 km/h and 45 km/h) falls while the lower back mostly

in 15 km/h falls. These similar fall kinematics were also observed in our previous findings.^{12,19} Although head injuries were predicted as the primary injuries during higher-speed snowboarding falls,^{19,20} the risk of back injuries can be still present. The tangential impact velocities of back-to-snow during falls of 35 km/h and 45 km/h were significantly higher than those during falls of 15 km/h. A higher tangential impact velocity might increase the body rotational movements, spinal flexions, and thus over-flexion-related SPI risks during falls. Higher SPI risks due to excessive spinal flexions were indeed observed in snowboarding backward falls at 35 km/h and 45 km/h than at 15 km/h.¹² The tangential impact velocity during snowboarding backward falls could also become the normal impact velocity during secondary impacts to a fixed obstacle after falls, for example. Therefore, the snowboarder with higher initial speeds might sustain higher impact energy and a higher possibility of back injuries under these conditions.

4.2 | Back injuries during back-to-snow impacts

The biomechanical responses of back-to-snow impacts were subsequently evaluated by applying the mean value

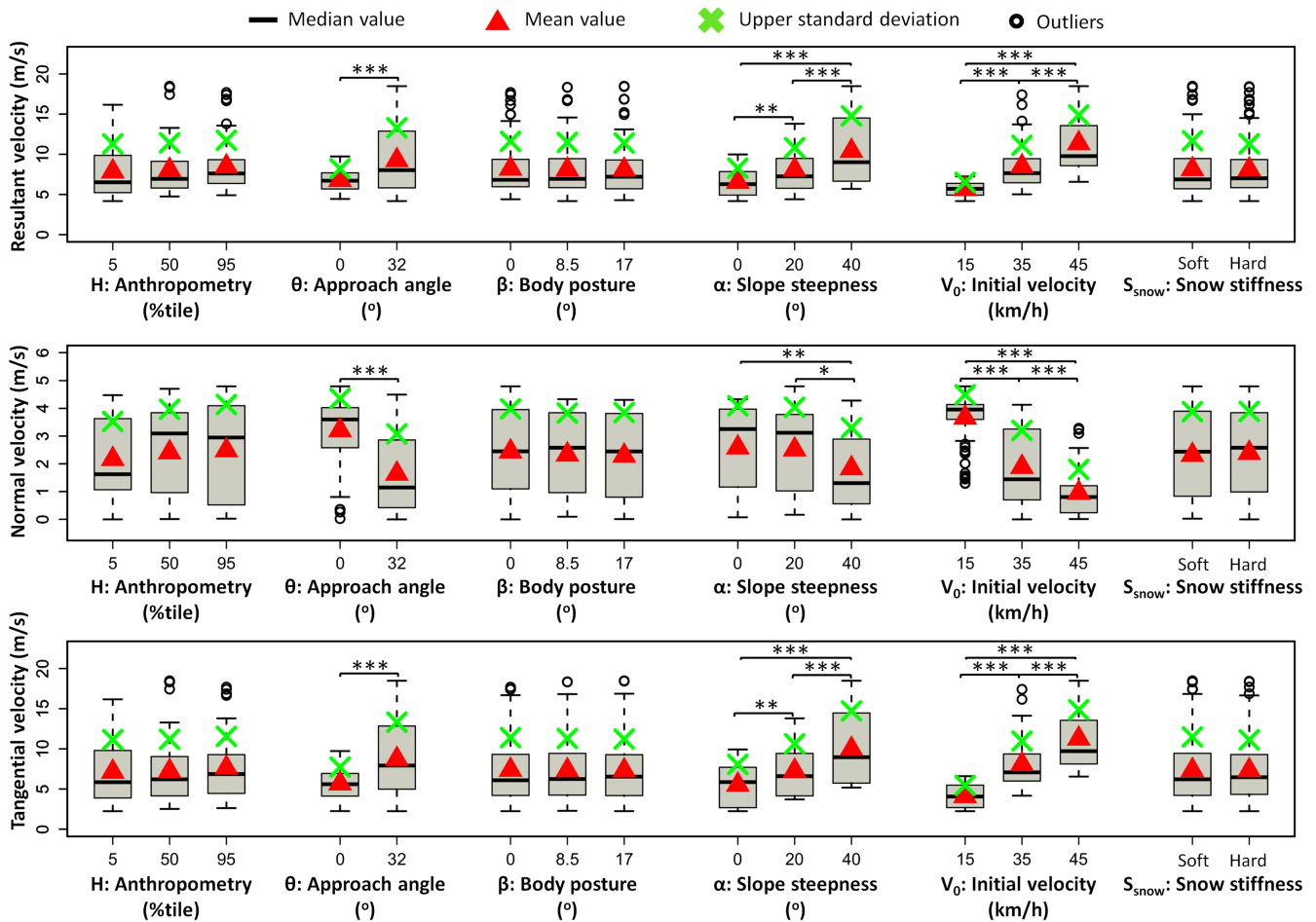


FIGURE 4 Back-to-snow impact velocity grouped by different levels of the initial condition variables. p values: *** $p < 0.001$, ** $p < 0.01$, * $p < 0.05$, $p < 0.1$

(2.4 m/s) of the normal back-to-snow impact velocity to the snowboarder FE model. The normalized ROM was higher in most thoracic FSUs than in lumbar FSUs (Figures D1 and D2 in Appendix D), not depending on the stiffness of the snow ground or the impacted position on the back. This suggested that the thoracic spine presented a higher risk of injury than the lumbar spine during back-to-snow impacts in terms of flexion-extension rotations. Similar predictions were also obtained in previous MB simulations of snowboarding backward falls.¹² The normalized ROM exceeded the injury threshold (100%) at the impacted FSUs or adjacent FSUs in impacts with the rigid bump surface: T8-T9 with the impact at T8, T12-L1 with the impact at T12 and L2. Inherently, T12-L1 had been already demonstrated as one of the most vulnerable spinal segments during snowboarding crashes.²⁹ In contrast, the normalized ROM was always below the injury threshold in impacts to the hard or soft snow, indicating less likely SPIs of excessive flexion-extension.

Vertebral fractures were also predicted using EPS at the impacted sites during impacts to the rigid floor and hard snow (Figure 6). The predicted vertebral fractures were

always located at the spinous process (3 cases at L1) and lamina (1 case at T9) regions. Gertzbein et al.³⁰ found that isolated spinous process fractures in the thoracic spine accounted for 4% of all thoracolumbar spinal fractures associated with skiing and snowboarding injuries. The posterior aspect of the spine hitting the ground was postulated as a leading mechanism of spinous process fractures in snowboarding or other sports.^{30,31} The spinous process fractures predicted at the impacted sites in this study also showed a good agreement with the previously postulated mechanism. Indeed, vertebral compression fractures constituted the majority (73.0–78.4%) of snowboarding-related thoracolumbar fractures,^{29,30} which were, however, not seen in the current back-to-snow impact simulations. One reason might be that the body rotational velocity and back-to-snow tangential impact velocity were not accounted for in the FE simulations. The body rotational velocity and back-to-snow tangential impact velocity might increase spinal flexions and induce vertebral compression fractures under the hyperflexion injury mechanism. Another reason was that the impact conditions causing a great level of spinal compression loading were not simulated in this study, for

TABLE 2 The peak values of the back-to-snow impact force and the back compression measured respectively at the T8, T12, L2, and L4 levels for the backward falls on the rigid floor, hard and soft snow with a flat impact surface or a spherical bump impact surface at the T8 (Sph-T8), T12 (Sph-T12), L2 (Sph-L2), and L4 (Sph-L4) levels

Material	Impact surface	Back compression (%)				Impact force (kN)
		T8 ^b	T12	L2	L4	
Rigid	Flat ^a	24.1	24.1	24.4	18.5	7.15
	Sph-T8 ^a	32.0	18.8	22.6	20.1	7.92
	Sph-T12 ^a	19.8	27.8	28.6	20.0	6.95
	Sph-L2 ^a	16.2	17.1	27.9	22.1	6.56
	Sph-L4 ^a	19.9	16.8	23.7	22.5	7.4
Hard Snow	Flat	21.1	19.9	21.8	17.8	5.85
	Sph-T8	25.5	18.9	22.2	18.8	6.18
	Sph-T12	20.8	23.8	24.9	17.8	5.91
	Sph-L2 ^a	18.6	19.8	24.1	19.6	5.75
	Sph-L4 ^a	19.0	19.9	21.7	16.9	5.8
Soft Snow	Flat ^a	18.6	17.6	21.3	15.4	5.06
	Sph-T8	21.9	17.2	20.0	17.1	5.14
	Sph-T12 ^a	18.7	20.0	22.1	16.1	5.23
	Sph-L2 ^a	17.1	18.4	21.5	16.1	5.25
	Sph-L4	17.4	18.2	20.3	14.9	5.27

^aAt least one rib was fractured in the corresponding cases.

^bA chest compression of 25.3% (and 22.0%) measured at T8 corresponds to a 50% (and 25%) probability of AIS2+ thoracic injuries.²¹

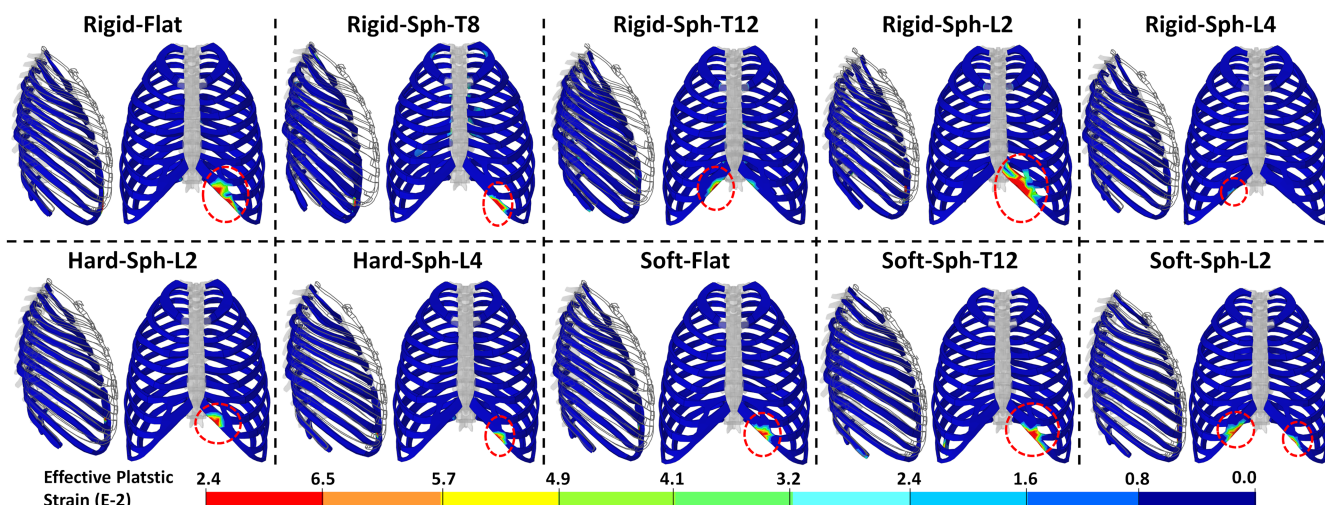


FIGURE 5 The effective plastic strain of the rib cage cortical bones to show the simulations with fractures and the corresponding fractured sites: the red cycles indicate the fractured sites on the rib cage and the gray lines on the lateral profile image show the original contour of the rib cage before deformation

example, when the head hit the snow ground first with a 45° angle between the body and ground. Closed head injuries were indeed found as the most common concomitant injuries with SPIs.³²

Apart from SPIs, chest injuries were also predicted in back-to-snow impacts. The back compression measured at the T8 level was up to 25.5% and 21.9% during impacts to the hard and soft snow (Table 2). The back compressions corresponded respectively to a 51% and 21.9% risk of AIS2+ injuries according to the injury risk curves in

terms of the THUMS model mid-thorax compressions.²¹ Rib cage fractures were indeed predicted using EPS in the current study during impacts to the hard and soft snow (Table 2 and Figure 5). All the fractures were found at the lower level of the costal cartilages which collided with the diaphragm and the abdominal organs during thoracoabdominal compression. Rib fractures accounted for 55.2% of snowboarding-related chest injuries.³³ Costal cartilage fractures were also reported in snowboarding-related injuries.^{34,35} Nevertheless, the frequency of rib or costal

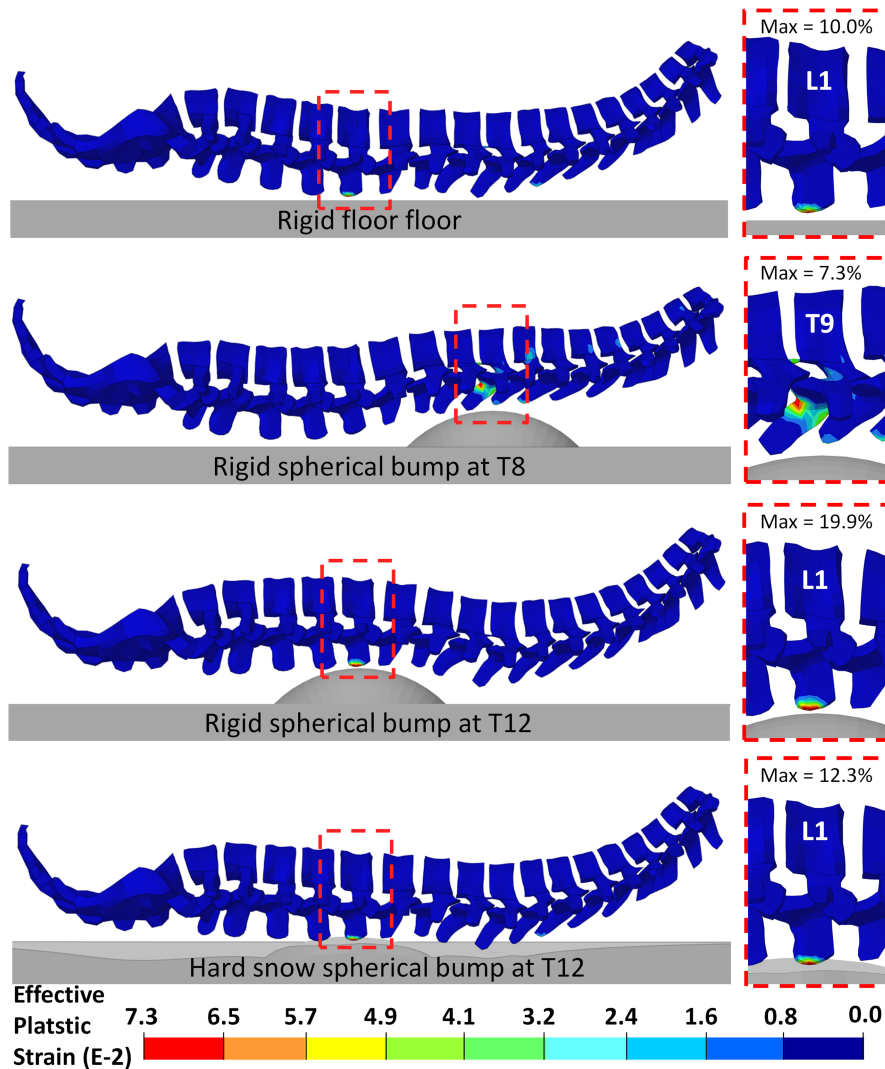


FIGURE 6 The effective plastic strain of the cortical bones of the spinal vertebrae to show the simulations with vertebral fractures and the corresponding fractured segments

cartilage fractures resulting from a blunt impact to the back in snowboarding was not available in the literature.

Three levels of “snow” stiffness were simulated in back-to-snow impacts. Unsurprisingly, the biomechanical loadings to the back increased with the increasing stiffness of the impact surface (i.e. soft snow < hard snow < rigid floor). In more detail, the impacted FSU (e.g. T8-T9 in back-to-snow impacts at T8) always had a higher normalized ROM on the stiffer impact surface, which was nevertheless not always true for other FSUs. The back compression measured at the impacted FSUs, the peak EPS of spinal cortical bones, and the back-to-snow impact force were always higher on the stiffer impact surface. To be noted, the impact forces of the back to the rigid floor, hard and soft snow was only up to 7.92 kN, 6.18 kN, and 5.27 kN respectively. Although these impact forces were much lower than the force thresholds (24 kN for level 1 and 12 kN for level 2) of a single strike in the current BPD testing standard,⁸ possible back injuries including vertebral and rib cage fractures were predicted in back-to-snow impacts. This might provide additional biomechanical

knowledge for the improvement of the current BPD testing: to increase the testing impact energy (e.g. impact velocity or impactor mass) and/ or to reduce the force evaluation thresholds to more reasonable values.

4.3 | Limitation

Several limitations of this study still need to be noted. The biomechanical responses during back-to-snow impacts did not consider the effects of the back-to-snow tangential impact velocity. The reasons for this compromise were twofold: firstly, the THUMS model was validated against blunt impacts to the back only with normal impact velocities and the model bio-fidelity was not warranted under impact conditions with shear effects (tangential velocity) to the back; secondly, the material properties of the snow were only characterized under normal impact velocities and might not be valid under a considerable level of shear loadings. Another limitation is that only one back-to-snow impact velocity

was simulated: 2.4 m/s, the mean value of the normal impact velocity obtained from MB simulations. The biomechanical responses shall be further evaluated with the range of back-to-snow impact velocities obtained in our snowboarding fall MB simulations. Muscle activation levels are uncertain during snowboarding falls and thus the active musculature of the THUMS model was turned off in this work. It could be interesting to evaluate the effect of active musculature on back injury risks in snowboarding falls in our following studies. This was the first study on snowboarding back injuries with FE modeling and we chose to study the effect of the impact surface features (stiffness and shape) on injury risks. However, other crash parameters (e.g. the pre-crash body posture, the dimensions of the bump impact surface) could influence back injury mechanisms or risks, and thus remain to be evaluated in future works.

5 | PERSPECTIVES

This study evaluated the back-to-snow impact conditions and the associated injury mechanisms during typical snowboarding backward falls. The normal and tangential back-to-snow impact velocities were found on average 2.4 m/s and 7.3 m/s respectively. The upper back was found more likely to hit the snow first, but the lower back hit the snow with a higher normal impact speed. The injury risk associated with excessive flexion-extension ROMs was higher in the thoracic spine than in the lumbar spine. Vertebral and rib cage fractures were predicted at the posterior elements of the vertebrae and the costal cartilage during back-to-snow impacts. Despite the possible back injuries, the back-to-snow impact force was always lower than the force thresholds of the current BPD testing standard. The current work may provide additional biomechanical knowledge for the future design of back protections, especially for snowboarders.

CONFLICT OF INTEREST

None.

DATA AVAILABILITY STATEMENT

The data that supports the findings of this study are available in the supplementary material of this article.

REFERENCES

- Statista. Hamburg (DE): Statista. <https://www.statista.com>. 2020, n.d. Accessed April 21, 2020.
- National Ski Areas Association. Active domestic skiers/snowboarders, 1996/97 to 2017/18. http://www.nsaa.org/media/341889/Number_of_participants_by_equipment.pdf. Accessed November 1, 2020.
- Weinstein S, Khodae M, VanBaak K. Common skiing and snowboarding injuries. *Curr Sports Med Rep*. 2019;18:394-400.
- bfu-Swiss Council for Injury Prevention. STATUS 2017: STATUS 2017. Statistics on non-occupational accidents and the level of safety in Switzerland. <https://www.bfu.ch>. Accessed June 15, 2020.
- Yamakawa H, Murase S, Sakai H, et al. Spinal injuries in snowboarders: risk of jumping as an integral part of snowboarding. *J Trauma Acute Care Surg*. 2001;50:1101-1105.
- Corra S, Girardi P, de Giorgi F, Braggion M. Severe and polytraumatic injuries among recreational skiers and snowboarders: incidence, demographics and injury patterns in South Tyrol. *Eur J Emerg Med*. 2012;19:69-72.
- White NH, Black NH. Spinal cord injury facts and figures at a glance. Natl Spinal Cord Inj Stat Cent Facts Fig Glance Birm AL Univ Ala Birm. 2017. Accessed May 15, 2020. <https://www.nscisc.uab.edu/Public/Facts%20and%20Figures%20-%202017.pdf>
- EN 1621-2 - Protective clothing against mechanical shock for motorcyclists - Part 2: back protectors - Requirements and test methods; 2014.
- Michel FI, Schmitt KU, Liechti B, Stämpfli R, Brühwiler P. Functionality of back protectors in snow sports concerning safety requirements. *Eng Sport 8 - Eng Emot*. 2010;2:2869-2874.
- Schmitt KU, Liechti B, Michel FI, Stämpfli R, Brühwiler PA. Are current back protectors suitable to prevent spinal injury in recreational snowboarders? *Br J Sports Med*. 2010;44:822-826.
- Signetti S, Nicotra M, Colonna M, Pugno NM. Modeling and simulation of the impact behavior of soft polymeric-foam-based back protectors for winter sports. *Snow Sports Trauma Saf 22nd Congr*. 2019;22:S65-S70.
- Wei W, Evin M, Bailly N, Llari M, Laporte JD, Arnoux PJ. Spinal injury analysis for typical snowboarding backward falls. *Scand J Med Sci Sports*. 2019;29:450-459.
- Poulard D, Kent RW, Kindig M, Li Z, Subit D. Thoracic response targets for a computational model: a hierarchical approach to assess the biofidelity of a 50th-percentile occupant male finite element model. *J Mech Behav Biomed Mater*. 2015;45:45-64.
- Siegel JH, Belwadi A, Smith JA, Shah C, Yang K. Analysis of the mechanism of lateral impact aortic isthmus disruption in real-life motor vehicle crashes using a computer-based finite element numeric model: with simulation of prevention strategies. *J Trauma Acute Care Surg*. 2010;68:1375-1395.
- Wei W, Kahn CJF, Behr M. Fluid-structure interaction simulation of aortic blood flow by ventricular beating: a preliminary model for blunt aortic injuries in vehicle crashes. *Int J Crashworthiness*. 2020;25:299-306.
- Brolin K, Wass J. Explicit finite element methods for equestrian applications. *Eng SPORT*. 2016;11(147):275-280.
- Li J, Chen D, Tang X, Li H. On the protective capacity of a safety vest for the thoracic injury caused by falling down. *Biomed Eng Online*. 2019;18:40.
- Scher I, Richards D, Carhart M. Head injury in snowboarding: evaluating the protective role of helmets. *J ASTM Int*. 2006;3:14203-14209.
- Bailly N, Abouchiche S, Masson C, Donnadiou T, Arnoux PJ. Recorded speed on alpine slopes: how to interpret Skier's perception of their speed? In: Scher IS, Greenwald RM, Petrone N, eds. *Snow Sports Trauma and Safety*. Springer; 2017:163-174.

20. Bailly N, Llari M, Donnadiou T, Masson C, Arnoux PJ. Head impact in a snowboarding accident. *Scand J Med Sci Sports*. 2017;27:964-974.
21. Mendoza-Vazquez M, Jakobsson L, Davidsson J, Brodin K, Östmann M. Evaluation of thoracic injury criteria for THUMS finite element human body model using real-world crash data. *IRCOBI Conference Proceedings, 10–12 September, Berlin, Germany, 2014; (IRC-14-62):528-541*. Accessed July 10, 2021. <http://www.ircobi.org/w>
22. Golman AJ, Danelson KA, Miller LE, Stitzel JD. Injury prediction in a side impact crash using human body model simulation. *Accid Anal Prev*. 2014;64:1-8.
23. Iwamoto M, Nakahira Y, Kimpara H. Development and validation of the Total HUMAN model for safety (THUMS) toward further understanding of occupant injury mechanisms in Pre-crash and during crash. *Traffic Inj Prev*. 2015;16:S36-S48.
24. Viano DC, Hardy WN, King AI. Response of the head, neck and torso to pendulum impacts on the Back. *J Crash Prev Inj Control*. 2001;2:289-306.
25. Forman J, Perry B, Henderson K, et al. Blunt impacts to the back: biomechanical response for model development. *J Biomech*. 2015;48:3219-3226.
26. Sterba M, Aubin CÉ, Wagnac E, Fradet L, Arnoux PJ. Effect of impact velocity and ligament mechanical properties on lumbar spine injuries in posterior-anterior impact loading conditions: a finite element study. *Med Biol Eng Comput*. 2019;57:1381-1392.
27. de Roulet A, Inaba K, Strumwasser A, et al. Severe injuries associated with skiing and snowboarding: a national trauma data bank study. *J Trauma Acute Care Surg*. 2017;82:781-786.
28. Bigdon SF, Gewiess J, Hoppe S, et al. Spinal injury in alpine winter sports: a review. *Scand J Trauma Resusc Emerg Med*. 2019;27:1-11.
29. Hosaka N, Arai K, Otsuka H, Kishimoto H. Incidence of recreational snowboarding-related spinal injuries over an 11-year period at a ski resort in Niigata, Japan. *BMJ Open Sport Amp Exerc Med*. 2020;6:e000742.
30. Gertzbein SD, Khoury D, Bullington A, John TA, Larson AI. Thoracic and lumbar fractures associated with skiing and snowboarding injuries according to the AO Comprehensive classification. *Am J Sports Med*. 2012;40:1750-1754.
31. Upadhyaya GK, Shukla A, Jain VK, Sinha S, Arya RK, Naik AK. Contiguous multiple cervicothoracic spinous process fractures in an adult: a case report. *J Clin Orthop Trauma*. 2016;7:45-49.
32. Hubbard ME, Jewell RP, Dumont TM, Rughani AI. Spinal injury patterns among skiers and snowboarders. *Neurosurg Focus FOC*. 2011;31:E8.
33. Machida T, Hanazaki K, Ishizaka K, et al. Snowboarding injuries of the chest: comparison with skiing injuries. *J Trauma Acute Care Surg*. 1999;46:1062-1065.
34. Sollender GE, White TW, Pieracci FM. Fracture of the costal cartilage: presentation, diagnosis, and management. *Ann Thorac Surg*. 2019;107:e267-e268.
35. Kerr H, Bowen B, Light D. Thoracoabdominal injuries. In: Micheli LJ, Purcell L, eds. *Adolesc Athlete Pract Approach*. Springer; 2018:113-133.

SUPPORTING INFORMATION

Additional supporting information can be found online in the Supporting Information section at the end of this article.

How to cite this article: Wei W, Evin M, Bailly N, Arnoux P-J. Biomechanical evaluation of Back injuries during typical snowboarding backward falls. *Scand J Med Sci Sports*. 2023;33:224-234. doi: [10.1111/sms.14254](https://doi.org/10.1111/sms.14254)